IAC-08-A1.4.06

MONTE CARLO SIMULATIONS OF ENERGY LOSSES BY SPACE PROTONS IN THE CRaTER DETECTOR

Lawrence W. Townsend
The University of Tennessee, Knoxville, Tennessee, United States of America
ltownsen@tennessee.edu

Hanna M. Moussa
The University of Tennessee, Knoxville, Tennessee, United States of America
hmoussa@utk.edu

Youssef M. Charara
The University of Tennessee, Knoxville, Tennessee, United States of America
ycharara@utk.edu

ABSTRACT

The Cosmic Ray Telescope for the Effects of Radiation (CRaTER) detector is to be carried on the Lunar Reconnaissance Orbiter (LRO) spacecraft, which scheduled for launch in early 2009. In lunar orbit, CRaTER will be used to help characterize the lunar radiation environment and its biological impacts on humans. The aim of this work is to estimate the energy lost and the linear energy transfer (LET) in CRaTER from energetic protons, such as those found in solar energetic particle events and galactic cosmic ray environments. Simulations of CRaTER component responses to protons with energies between 100 MeV and 2 GeV are made using the recently-modified HETC-HEDS Monte Carlo radiation transport code and presented for each component in the detector stack. As a check on the validity of these results obtained from HETC-HEDS, energy loss and LET spectra for protons at incident energies of 300, 600 and 1000 MeV are obtained using the Monte Carlo Code System for Multiparticle and High Energy Applications (MCNPX) and compared with the HETC-HEDS predictions. Agreement between the predictions from these two codes for a variety of proton energies between 300 and 2000 MeV is found to be within approximately 10%.

INTRODUCTION

The Cosmic Ray Telescope for the Effects of Radiation (CRaTER) detector is to be carried on the Lunar Reconnaissance Orbiter (LRO) spacecraft, which scheduled for launch in early 2009. The LRO mission is the first in a planned series of robotic missions to Earth's moon. The spacecraft will orbit the Moon in a polar orbit, at an altitude of 50 km, for a nominal one-year mission. In lunar orbit, CRaTER will be used to help characterize the lunar radiation environment and its biological impacts on humans. Other LRO objectives include: (1) developing a high-resolution global, three-

dimensional geodetic grid of the Moon and provide the topography necessary for selecting future landing sites; (2) assessing in detail the resources and environments of the Moon's polar regions; and (3) conducting a high spatial resolution assessment of the Moon's surface including addressing elemental composition, mineralogy, and regolith characteristics. Details of the other instruments selected to meet these other objectives are presented elsewhere [1].

The aim of this work is to estimate the energy lost and the linear energy transfer in CRaTER from energetic protons, such as those found in solar energetic particle (SEP) events and galactic cosmic ray environments. Simulations of detector responses to protons with energies between 100 MeV and 2 GeV are made using the recently-modified HETC-HEDS (High Energy Transport Code – Human Exploration and Development of Space) Monte Carlo radiation transport code [2]. These proton energies span the range of SEP protons detectable by CRaTER. Currently, calibration of the detector is being carried out using proton beams from the cyclotron at Massachusetts General Hospital, beams of protons and heavy ions from the LBNL 88' cyclotron, and Fe beams obtained at the NASA Space Radiation Laboratory (NSRL) at BNL. Simulations of these calibration runs are underway, as are data analyses from the calibration runs themselves. These will be reported in the future, when completed. As a check on the validity of the results obtained from HETC-HEDS, energy loss and LET spectra for protons at incident energies of 300, 600 and 1000 MeV are obtained using the Monte Carlo Code System for Multiparticle and High Energy Applications (MCNPX) [3] and compared with the HETC-HEDS results.

CRaTER DETECTOR DESCRIPTION

CRaTER was designed and built by a team of researchers and engineers from Boston University, Massachusetts Institute of Technology, Aerospace Corporation, and the University of Tennessee. The detector configuration is depicted in Fig. 1.

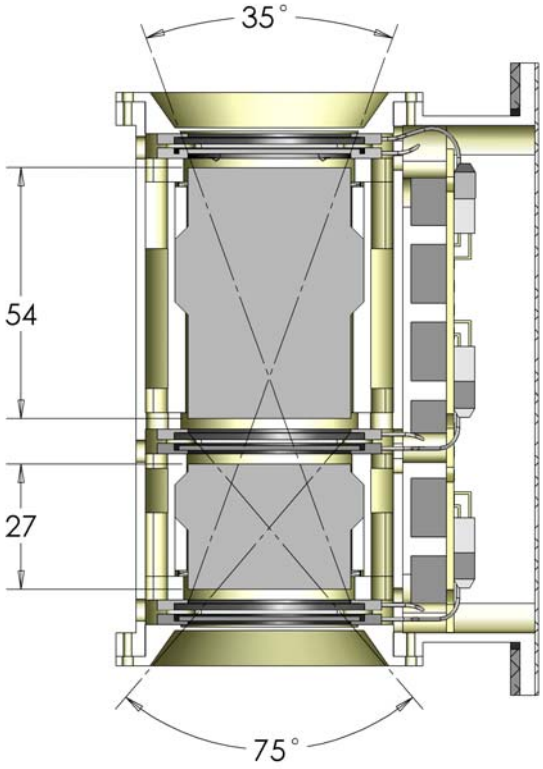

Fig. 1: CRaTER detector configuration. The A-150 tissue equivalent plastic sections are labeled 54 (5.4 cm length) and 27 (2.7 cm length) in the figure. The silicon detector pairs are located above the top A-150 section, below the bottom A-150 section, and between them.

The detector consists of a stack of silicon detectors and tissue-equivalent plastic (TEP) to measure the linear energy transfer (LET) spectra of cosmic radiation relevant for human and electronic parts considerations. It is embedded within thin cylindrical aluminum housing, the top and bottom thickness of aluminum housing is 0.0762 cm and the side thickness is 0.1524 cm. The

detector stack consists of six silicon detectors divided into three pairs. Each pair consists of a thin detector (nominally 140μm thickness) and a thick detector (nominal 1mm thickness). The thin detectors are designed to measure energy losses from energetic heavy ions (2 MeV threshold) and the thick detectors from protons (0.2 MeV threshold). Sandwiched between each pair of detectors is a section of A-150 tissue-equivalent plastic (TEP), which is used to provide the tissue-equivalent medium for measuring LET. Starting with the zenith end of the detector stack (35 degrees field of view (FOV) for 6 detector coincidences), which faces out into space, and working toward the nadir end (75 degrees FOV for bottom 4 detector coincidences), which faces the lunar surface, there is a silicon detector pair (D1-D2), then 5.4 cm of A-150 TEP, then another detector pair (D3-D4), followed by 2.7 cm of A-150 TEP, and the final detector pair (D5-D6). D1, D3 and D5 are the thin detectors. D2, D4 and D6 are the thick detectors. The actual detector radii are 1.7485 cm.

Once the LRO mission begins, LET measurements in the TEP sections will be obtained using

$$LET = \frac{dE}{dx} = \frac{E_0 - E_f}{L}$$

where E_0 and E_f are the energies of the particles as measured by the silicon detectors at either end of each TEP section and L is the length of the TEP section.

MONTE CARLO SIMULATIONS

Simulations of the passage of high-energy space protons through the CRaTER detector stack were carried out using the HETC-HEDS [2] and MCNPX [3] Monte Carlo radiation transport codes. The earlier version of HETC [4] simulates the particle cascade by using Monte Carlo techniques to compute the trajectories of the primary particle and the secondary particles produced in nuclear collisions. The particles considered by the earlier version of HETC (protons, neutrons, π^+, π^-, μ^+, or μ^-) could be arbitrarily distributed in angle, energy, and space. HETC used the combinatorial geometry package so virtually arbitrary geometries are allowed. Each particle in the cascade is followed until it eventually disappears by escaping from the geometric boundaries of the system, undergoes nuclear collision or absorption, comes to rest due to energy losses from ionization and excitation of atomic electrons, or, in the case of pions and muons, decays. Neutrons produced below a given cutoff, usually 20 MeV, and photons produced in the cascade or from deexcitation gammas are not transported. Instead, the information is stored for transport by other codes such as MORSE [5]. A complete cascade history tape is provided by HETC and HETC-HEDS. Not included in the original HETC was the transport of particles with A > 1. HETC has been modified to include the transport of heavier nuclei [2], [6]. Included in this newer version of HETC, now called HETC-HEDS, are nucleus-nucleus cross sections, range-energy tables scaled from the proton data, and a nuclear collision module for heavy ion interactions.

For the HETC-HEDS calculations in this work, incident proton energies between 100 MeV and 2 GeV were used. For validation of the HETC-HEDS results, three high-energy proton beams were used in the MCNPX simulation with energies of 1 GeV, 600 MeV and 300 MeV. Each beam is uniformly and normally incident on the entire surface of the detector on the zenith side (D1). In addition, only events where the particles incident on the front surface of the

TEP element and exiting the back surface are used to calculate the energy deposition in the TEP element, since this simulates the actual methodology that will be used during the LRO mission to measure LET. For the HETC-HEDS runs, particle fluences and energy deposition in each component were calculated. In the MCNPX runs the average energy lost per incident proton in each detector element is estimated. For each incident proton energy, up to 1 million histories were used in the HETC-HEDS runs. For the MCNPX runs, 512K histories were used. The energy losses per proton incident on the TEP element are then divided by the thickness of each detector to obtain the tissue equivalent LET values.

RESULTS

Table 1 displays the relative fluences (normalized per incident proton) exiting each component and energy depositions in each detector component calculated using the HETC-HEDS code. Results are presented for protons (incident and secondary) and for other secondary particles (all other secondaries except protons; mainly contributions from neutrons).

Note that incident protons with energies of l00 MeV cannot penetrate the entire length of the detector stack. Note also that as the incident proton energies increase, the relative proton fluence may slightly exceed unity for the first few components in the detector stack due to the presence of secondary protons produced by spallation or fragmentation reactions in these components. The relative fluences of other secondary particles exiting each component are fairly low since heavy target recoils and fragments have ranges that are far too small to exit a component unless they are produced very near the exiting surface.

From Table 1 we note that the energy losses per incident proton in the TEP segments are between 7 and 61 MeV for protons; whereas, for the secondaries, which exclude protons, the energy losses per incident proton in the TEP segments are less than 0.1 MeV for incident protons with energies 1000 MeV and lower, and less than 0.15 MeV for incident protons with energies of 2000 MeV. Hence, contributions to the measured LET spectrum for solar energetic particle events from secondary particles other than protons should be relatively small ($\leq$ 1-2%) for this detector.

Linear Energy Transfer (LET) values for protons (primary and secondary) for each of the two A-150 TEP components are displayed in Figs. 2 and 3 as a function of incident proton energy. The values for the 5.4 cm TEP element are displayed in Fig. 2 and values for the 2.7 cm TEP element are displayed in Fig.3. Plotted are LET calculations obtained from HETC-HEDS for incident proton energies from 200 MeV to 1000 MeV in steps of 100 MeV. For clarity in comparing the two sets of calculations, values for protons having incident energies of 100 and 2000 MeV are not plotted, but are calculated to be 11.4 and 2.67 MeV/cm for the 5.4 cm element, and 10.2 and 2.60 MeV/cm for the 2.7 cm element. Also plotted are LET calculations obtained from the MCNPX code for incident proton energies of 300, 600 and 1000 MeV. Values for 2000 MeV were not estimated using MCNPX since it has much longer running times than HETC-HEDS. Typically, running times needed to generate the cascade history file for 100,000 histories using HETC-HEDS were <10 minutes on a personal computer. Note that the calculated LET values were nearly the same for either TEP elements. Differences were only ~2% between the estimates for the two elements.

Component	Protons		Other Secondaries	
	Relative Fluence	Energy Deposited (MeV)	Relative Fluence	Energy Deposited (MeV)
		100 MeV		
D1	1.000	0.208	0	0
D2	0.999	1.415	0	0
A1	0.918	61.303	0	0
D3	0.917	0427	0	0
D4	0.912	2.972	0	0
A2	0.000	27.496	0	0
D5	0.000	0.000	0	0
D6	0.000	0.000	0	0
		200 MeV		
D1	1.001	0.129	0	0
D2	1.000	0.882	0	0
A1	0.961	29.592	0	0
D3	0.957	0.141	0	0
D4	0.952	0.945	0	0
A2	0.922	15.430	0	0
D5	0.913	0.143	0	0
D6	0.910	0.958	0	0
		300 MeV		
D1	1.001	0.103	2.20E-05	1.02E-06
D2	1.001	0.700	3.50E-05	5.63E-05
A1	0.967	22.585	5.50E-05	3.31E-04
D3	0.963	0.106	3.20E-05	1.23E-06
D4	0.957	0.708	2.40E-05	1.67E-05
A2	0.929	11.195	2.90E-05	1.52E-04
D5	0.918	0.103	1.50E-05	9.00E-08
D6	0.915	0.690	1.30E-05	1.07E-05
		400 MeV		
D1	1.001	0.089	1.63E-04	7.62E-06
D2	1.002	0.608	2.22E-04	2.24E-04
A1	0.969	19.451	5.64E-04	3.28E-03
D3	0.964	0.090	3.51E-04	5.21E-06
D4	0.959	0.615	2.99E-04	1.42E-04
A2	0.930	9.483	3.02E-04	1.55E-03
D5	0.918	0.087	1.79E-04	1.07E-06
D6	0.915	0.588	1.79E-04	6.80E-05
		500 MeV		
D1	1.002	0.081	5.17E-04	1.72E-05
D2	1.002	0.561	6.85E-04	6.41E-04
A1	0.971	17.815	1.97E-03	1.02E-02
D3	0.965	0.083	1.20E-03	1.62E-05
D4	0.960	0.559	1.03E-03	3.06E-04
A2	0.929	8.605	1.24E-03	5.58E-03
D5	0.915	0.079	7.32E-04	5.43E-06
D6	0.912	0.530	6.99E-04	2.09E-04
		600 MeV		
D1	1.003	0.078	9.38E-04	1.60E-05
D2	1.003	0.535	1.27E-03	1.05E-03
A1	0.973	16.896	4.51E-03	2.21E-02
D3	0.967	0.078	2.92E-03	3.21E-05
D4	0.961	0.543	2.51E-03	5.05E-04
A2	0.928	8.119	2.82E-03	1.18E-02
D5	0.913	0.074	1.65E-03	1.10E-05
D6	0.910	0.508	1.56E-03	3.00E-04
		700 MeV		
D1	1.003	0.075	1.27E-03	3.39E-05
D2	1.004	0.516	1.82E-03	1.45E-03
A1	0.975	16.310	7.31E-03	3.56E-02
D3	0.969	0.076	5.06E-03	3.87E-05
D4	0.963	0.526	4.38E-03	6.31E-04
A2	0.928	7.839	5.11E-03	2.02E-02
D5	0.912	0.074	3.10E-03	2.69E-05
D6	0.909	0.499	2.90E-03	4.32E-04
		800 MeV		
D1	1.004	0.073	1.64E-03	4.52E-05
D2	1.005	0.508	2.33E-03	1.84E-03
A1	0.977	15.807	9.41E-03	4.52E-02
D3	0.971	0.073	6.67E-03	5.18E-05
D4	0.965	0.503	5.87E-03	6.55E-04
A2	0.929	7.602	6.72E-03	2.64E-02
D5	0.913	0.069	4.21E-03	3.32E-05
D6	0.910	0.481	3.99E-03	4.49E-04
		900 MeV		
D1	1.004	0.072	1.82E-03	6.94E-05
D2	1.005	0.491	2.54E-03	1.73E-03
A1	0.979	15.464	1.10E-02	5.22E-02
D3	0.972	0.072	7.86E-03	8.12E-05
D4	0.967	0.509	7.01E-03	7.66E-04
A2	0.931	7.426	8.05E-03	3.15E-02
D5	0.915	0.070	5.10E-03	3.52E-05
D6	0.912	0.462	4.82E-03	5.40E-04
		1000 MeV		
D1	1.004	0.070	2.08E-03	6.45E-05
D2	1.006	0.488	3.02E-03	2.17E-03
A1	0.981	15.115	1.28E-02	6.18E-02
D3	0.975	0.070	9.29E-03	8.81E-05
D4	0.969	0.498	8.31E-03	9.93E-04
A2	0.935	7.270	9.71E-03	3.79E-02
D5	0.918	0.068	6.24E-03	5.27E-05
D6	0.915	0.458	5.88E-03	5.27E-04
		2000 MeV		
D1	1.006	0.067	3.69E-03	1.04E-04
D2	1.009	0.466	5.55E-03	3.13E-03
A1	0.994	14.392	2.84E-02	1.39E-01
D3	0.988	0.067	2.28E-02	1.58E-04
D4	0.985	0.500	2.11E-02	1.65E-03
A2	0.961	7.025	2.38E-02	9.58E-02
D5	0.947	0.067	1.71E-02	1.45E-04
D6	0.945	0.478	1.65E-02	9.78E-04

Table 1: Relative fluence at component exit and energy deposition in each detector component as a function of incident proton energy obtained from HETC-HEDS.

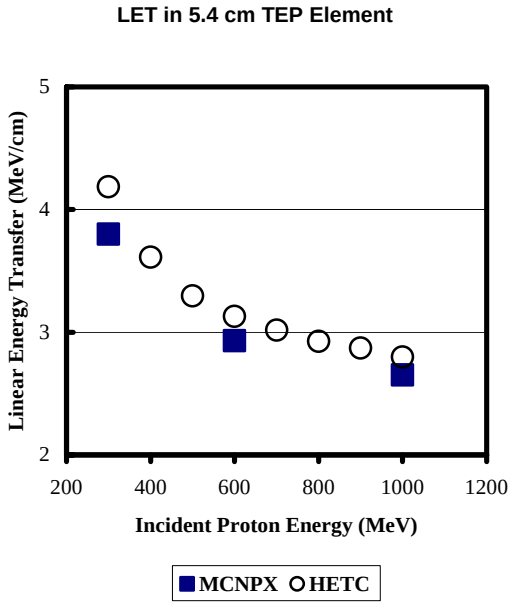

Fig. 2: Linear Energy Transfer in the 5.4 cm TEP element as a function of the energy of the protons incident on the element obtained from the HETC-HEDS and MCNPX codes.

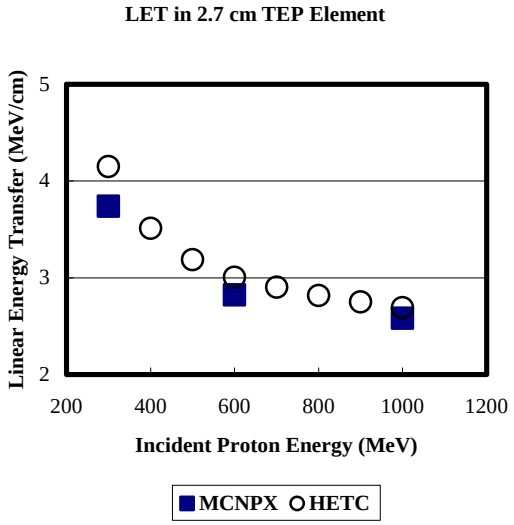

Fig. 3: Linear Energy Transfer in the 2.7 cm TEP element as a function of the energy of the protons incident on the element obtained from the HETC-HEDS and MCNPX codes.

Note that the agreement between the two sets of LET calculations is quite good. At an incident proton energy of 300 MeV, the difference is 10% for the 5.4cm TEP element and 11 % for the 2.7cm TEP element. As the incident proton energies increase, the differences are reduced. At an incident energy of 600 MeV, the differences are about 6.5% for both TEP elements. At an incident energy of 1000 MeV, the differences are 5.5% for the 5.4 cm element and 4.3% for the 2.7 cm element.

CONCLUSIONS

In this work we have used two Monte Carlo codes to simulate the energy losses and the LET in the two different volumes of tissue equivalent plastic detectors (TEP), within the CRaTER detector, for incident proton energies appropriate to studies of solar energetic particle events and galactic cosmic rays in deep space. The results obtained from HETC-HEDS can be used to characterize the detector response to incident SEP and GCR protons. Comparisons of the simulated results from HETC-HEDS and MCNPX indicate that the agreement between the code predictions is within ~10%.

REFERENCES

[1] http://lunar.gsfc.nasa.gov/missions/scandinst.html

[2] Lawrence W. Townsend, Thomas M. Miller, and Tony A. Gabriel, "HETC Radiation Transport Code Development for Cosmic Ray Shielding Applications in Space." Radiation Protection Dosimetry, Vol. 115, Nos. 1-4, December 2005, pp. 135-139.

[3] Gregg W. McKinney et al., "MCNPX Overview", LA-UR-06-6206 (278 KB), Proceedings of the 2006 HSSW, FNAL, IL, September 6-8, 2006.

[4] K. C. Chandler and T. W. Armstrong. *Operating instructions for the high-energy nucleon-meson transport code, HETC.* ORNL-4744, Oak Ridge National Laboratory, Oak Ridge, TN (1972).

[5] M. B. Emmett. *MORSE-CGA, a Monte Carlo radiation transport code with array geometry capability*. ORNL-6174 (April 1985).

[6] T. M. Miller and L. W. Townsend, "Comprehensive Cross Section Database Development for Generalized Three Dimensional Radiation Transport Codes." Nuclear Science and Engineering, Vol. 149, No. 1, January 2005, pp. 65-73.